Biomaterials 32 (2011) 2907–2917

Contents lists available at ScienceDirect

Biomaterials

journal homepage: www.elsevier.com/locate/biomaterials

Patterns of cancer invasion revealed by QDs-based quantitative multiplexed imaging of tumor microenvironment

Chun-Wei Peng [a], Xiu-Li Liu [a], Chuang Chen [a], Xiong Liu [a], Xue-Qin Yang [a], Dai-Wen Pang [b], Xiao-Bo Zhu [c], Yan Li [a,*]

[a] Department of Oncology, Zhongnan Hospital of Wuhan University, Hubei Key Laboratory of Tumor Biological Behaviors and Hubei Cancer Clinical Study Center, No. 169 Donghu Road, Wuchang District, Wuhan 430071, PR China
[b] Key Laboratory of Analytical Chemistry for Biology and Medicine (Ministry of Education), College of Chemistry and Molecular Sciences and State Key Laboratory of Virology, Wuhan University, Wuhan 430072, PR China
[c] Wuhan Jiayuan Quantum Dots Co., Ltd., and Wuhan Tumor Nanometer Diagnosis Engineering Research Center, Wuhan 430074, PR China

ARTICLE INFO

Article history:
Received 13 December 2010
Accepted 29 December 2010
Available online 22 January 2011

Keywords:
Quantum dots
Tumor microenvironment
Cancer invasion
Multiplexed imaging
Nanomedicine

ABSTRACT

Tumor growth and progression depends on their microenvironment, which undergoes constant co-evolution because of the dynamic tumor–stromal interactions. Such co-evolution has long been under appreciated due to the lack of appropriate technology platforms to simultaneously reveal these complex interactions. Here we report on a quantum dots based multiplexed imaging and spectrum analysis technology to simultaneously study major components of tumor stroma, including type IV collagen, tumor angiogenesis, macrophages infiltration and tissue destructive proteolytic enzyme matrix metalloproteinase 9. The new technology revealed a panoramic picture of the tempo-spatial co-evolution of tumor cells and their stroma at the architecture level. Four patterns of tumor invasion with distinctive co-evolution features were identified as Washing pattern, Ameba-like pattern, Polarity pattern and Linear pattern. This quantum dots based multiplexed technology could help gain new insight into the complex process of tumor invasion, and formulate new anti-cancer strategies.

1. Introduction

Invading tumor cells in vivo are confronted with three-dimensional (3D) extracellular matrix (ECM) networks that form physical barriers against the advancing cells [1]. Traditionally, invading depth is the center of attention, and few studies have concurrently focused on the dynamic co-evolution of the cancer cells and stroma. It has been recognized that invasion is regulated not only by intrinsic genetic changes in cancer cells as 'initiators' of carcinogenesis, but also by stromal cells as 'promoters' [2,3]. A seminal event in cancer progression is the ability of invading cells to migrate through tissue barriers particularly the basement-membrane, a specialized form of ECM that separates the epithelium from the stroma [4]. This process requires the co-evolution of cancer microenvironment that includes several simultaneous events, such as up-regulation and activation of proteolytic enzymes such as matrix metalloproteinases (MMPs), remodeling of ECM barrier (ECMB) mainly by cleaving and re-patterning type IV collagen, tumor angiogenesis, and recruitment and conversion of immune cells [5]. In recent years, the ECMB has been recognized as an important regulator of cell behavior, not only just a tissue structure scaffold. The ECMB mediates tissue compartmentalization and sends signals to epithelial cells about the external microenvironment [6]. Human cancer is especially complex because it evolves over a long time course and shows a multitude of molecular, cellular, and architectural heterogeneity [7,8]. Neither the studies at purely molecular and cellular levels, nor the studies at the purely clinical level can decipher the co-evolution of cancer microenvironment. At the architectural level, however, major critical molecular and cellular events and stroma changes can be visualized, revealing a real-time panoramic picture of the co-evolution of cancer cells and their microenvironment [9]. Unfortunately, such co-evolution of cancer microenvironment has long been under appreciated due to the lack of appropriate technology platforms to reveal the dynamic spatiotemporal processes.

Quantum dots (QDs) are engineered nanoparticles with unique optical and electronic properties which have potential applications ranging from medicine to energy [10,11]. Compared with organic

* Corresponding author. Tel.: +86 27 67813152; fax: +86 27 67812892.
E-mail address: liyansd2@163.com (Y. Li).

0142-9612/$ – see front matter © 2011 Elsevier Ltd. All rights reserved.
doi:10.1016/j.biomaterials.2010.12.053

dyes and fluorescent proteins, QDs have unique features such as size- and composition-tunable light emission, enhanced signal brightness, resistance to photobleaching [12–14]. In addition, different QDs colors can be simultaneously excited by a single light source, with minimal spectral overlapping, which provides significant advantages for multiplexed detection of targets. This property is very suitable for investigating the co-evolution of cancer cells and tumor microenvironment at the architectural level, a key issue in studying the

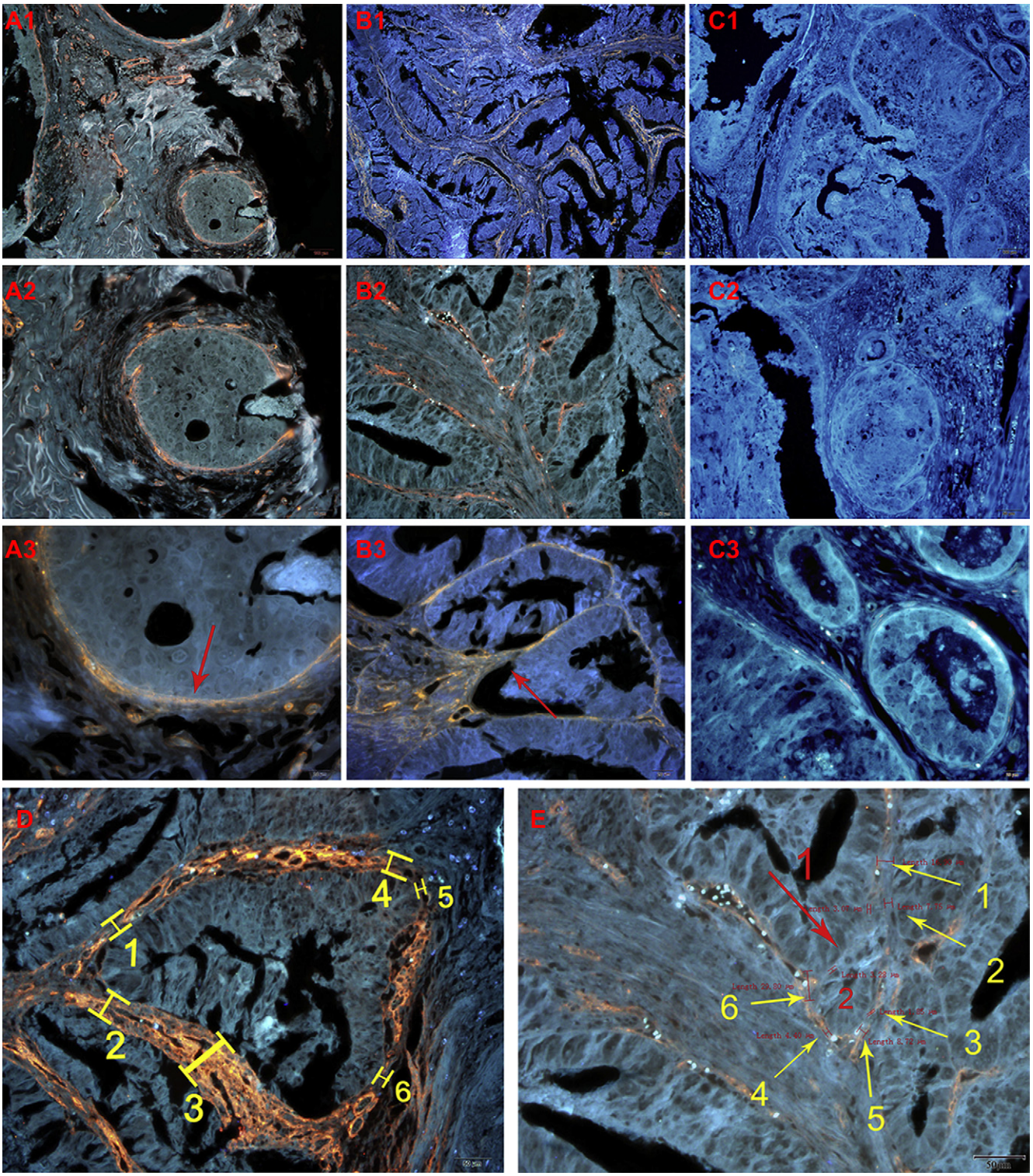

Fig. 1. Fluorescent imaging and quantitative analysis of ECMB in breast and gastric cancers. (A1–B3) Type IV collagen imaging in breast cancer (A1–A3) and gastric cancer (B1–B3) with QDs-585 probe. The spatial relationship between cancer cells and ECMB were indicated (red arrows). (C1–C3) Control slides without QDs staining. (D) A model demonstration of quantitative ECMB analysis. The thickness of ECMB at sites 1, 2, 3, 4, 5 and 6 is 18.23 μm, 29.88 μm, 63.52 μm, 24.71 μm, 9.07 μm and 10.54 μm, respectively. Diminished ECMB could be observed at the site of potential cancer invasion (site 5). (E) Actual performance of quantitative ECMB analysis, with serial numbers indicating the sites of measurement. The real thickness of ECMB at sites 1, 2, 3, 4, 5 and 6 is 16.90 μm, 7.75 μm, 1.85 μm, 8.72 μm, 4.40 μm and 29.80 μm, respectively. The ECMB between nest 1 and nest 2 is degraded at the invasion front (red arrow, 3.28 μm). Magnification: 100× (A1, B1, C1), 200× (A2, B2, C2, D, E), 400× (A3, B3, C3); Scale bar: 100 μm (A1, B1, C1), 50 μm (A2, B2, C2, D, E), 20 μm (A3, B3, C3).

mechanisms of cancer progression and also in developing more specific targeting therapeutic approaches [3,15–17].

In this work, we report on a new strategy to directly reveal the co-evolution of cancer cells and their microenvironment on human cancer tissues in order to gain better insights into the complex and dynamic biology of cancer invasion. Four common invasion patterns in 15 cases of gastric cancer specimens and 10 breast cancer specimens were revealed by QDs-based fluorescent imaging and spectrum analysis of type IV collagen. In addition, major components involved in the critical processes of cancer invasion were revealed simultaneously by multiplexed QDs imaging. This new multiplexed QDs mapping provides new spatiotemporal information on the co-evolution of cancer cells and microenvironment.

2. Materials and methods

2.1. Human cancer tissue specimens

Formalin-fixed paraffin-embedded tumor tissues from 15 gastric cancer patients and 10 breast cancer patients were obtained from the Department of Oncology, Zhongnan Hospital of Wuhan University (Wuhan, China). Tissue sections (4 μm thickness) were preheated at 60 °C for 1 h and were then de-paraffinized in xylene 3 times each for 5 min. Tissue hydration was carried out by a series of immersion steps at decreasing ethanol concentrations (100, 95, 95 and 85% ethanol for 5, 3, 3,

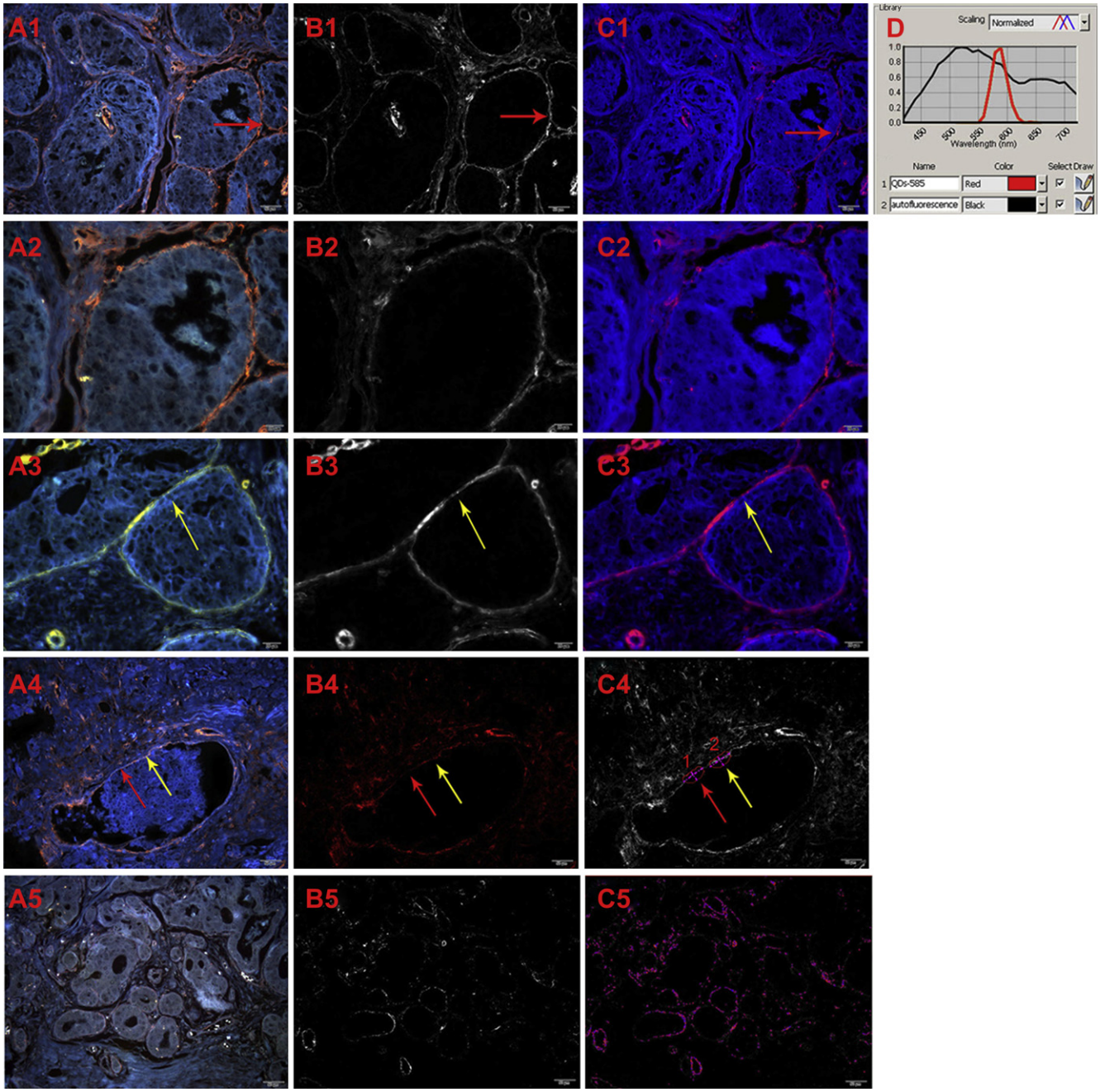

Fig. 2. Spectrum analysis and quantification of ECMB. (A1–A5) Fluorescent imaging. (B1–B5) Spectral signal of QDs-585 extracted from (A1–A5). (C1–C5) Corresponding unmixed image of (B1–B5), the colors of QDs were re-assigned to pseudocolors for graphic visualization or emphasis. (D) QD emission spectra and tissue autofluorescence data used for unmixed image. The continuity, smoothness and integrity of type IV collagen were displayed more clearly (Red arrows), and hiding points of ECMB broken were revealed (Yellow arrows). (C4) Signal quantification of whole slides. (C5) Signal quantification of ROI. Red arrows: area of ECMB degradation; Yellow arrows: ECMB intact area. Magnification: 200× (A1, B1, C1), 400× (A2–C5); Scale bar: 50 μm (A1, B1, C1), 20 μm (A2–C5).

and 3 min, respectively), followed by rinsing in water for 5 min. The slides were pretreated in 0.01 M citrate buffer (pH 6.0) and heated at 98 °C for 10 min for antigen retrieval. After cooling in the citrate buffer for another 25 min at room temperature, the tissue slides were washed in water and stored in 1× TBS plus buffer (containing 0.05% Tween 20) until use.

2.2. QDs-based immunohistochemical study of tumor microenvironment

The primary antibodies were rabbit anti-human polyclonal antibody against type IV collagen (ab-6586, Abcam, England, dilution 1/100), mouse anti-human monoclonal antibody against macrophages (MA1-38069, ABR, USA, dilution 1/200), goat anti-human polyclonal antibodies against MMP9 (sc-13595, Santa Cruz, USA, dilution 1/50) and CD105 (sc-20072, Santa Cruz, USA, dilution 1/50) for neovessels. The QDs probes were secondary antibodies conjugated with QDs on the $F(ab')_2$ fragments, including QDs-525 (QDs-525 goat $F(ab')_2$ anti-mouse IgG conjugate, Invitrogen, USA, dilution 1/100), QDs-585 (QDs-585 goat $F(ab')_2$ anti-rabbit IgG conjugate, Invitrogen, USA, dilution 1/100), QDs-655 (QDs-655 rabbit $F(ab')_2$ anti-goat IgG conjugate, Invitrogen, USA, dilution 1/100). The QDs-based immunofluorescent imaging of type IV collagen, macrophages, MMP9 and CD105 were conducted as previously described in prepared tissue slides [14]. For multiplexed QDs staining, a mixture of 3 primary antibodies from 3 species (e.g. mouse, rabbit and goat) was used to recognize 3 antigens in tissue sections. A mixture of 3 QDs probes was applied to stain the corresponding antibodies for 1 h at 37 °C.

2.3. Signal acquisition

The slides were examined under Olympus BX51 fluorescence microscope equipped with an Olympus DP72 camera (Olympus Optical Co., Ltd., Tokyo, Japan) and CRi Nuance multispectral imaging systems (Cambridge Research & Instrumentation, Inc., Woburn, MA, USA). The QDs-525, QDs-585 and QDs-655 were excited by ultraviolet light (330–385 nm). The QDs images were captured by DP72 camera. A spectral cube for each slide, which contains the complete spectral information at 10-nm wavelength intervals from 490 to 720 nm were collected by CRi Nuance systems. All the cubes were captured under the same condition at proper magnifications, which could make it more accurate and representative in tumor markers assay.

2.4. Spectrum analysis and biomarker quantification

Deconvolution algorithms were applied to image each cube, generating a set of "single-color" images representing each individual QDs/biomarker and the tissue autofluorescence. The QDs colors were converted to pseudocolors for graphic

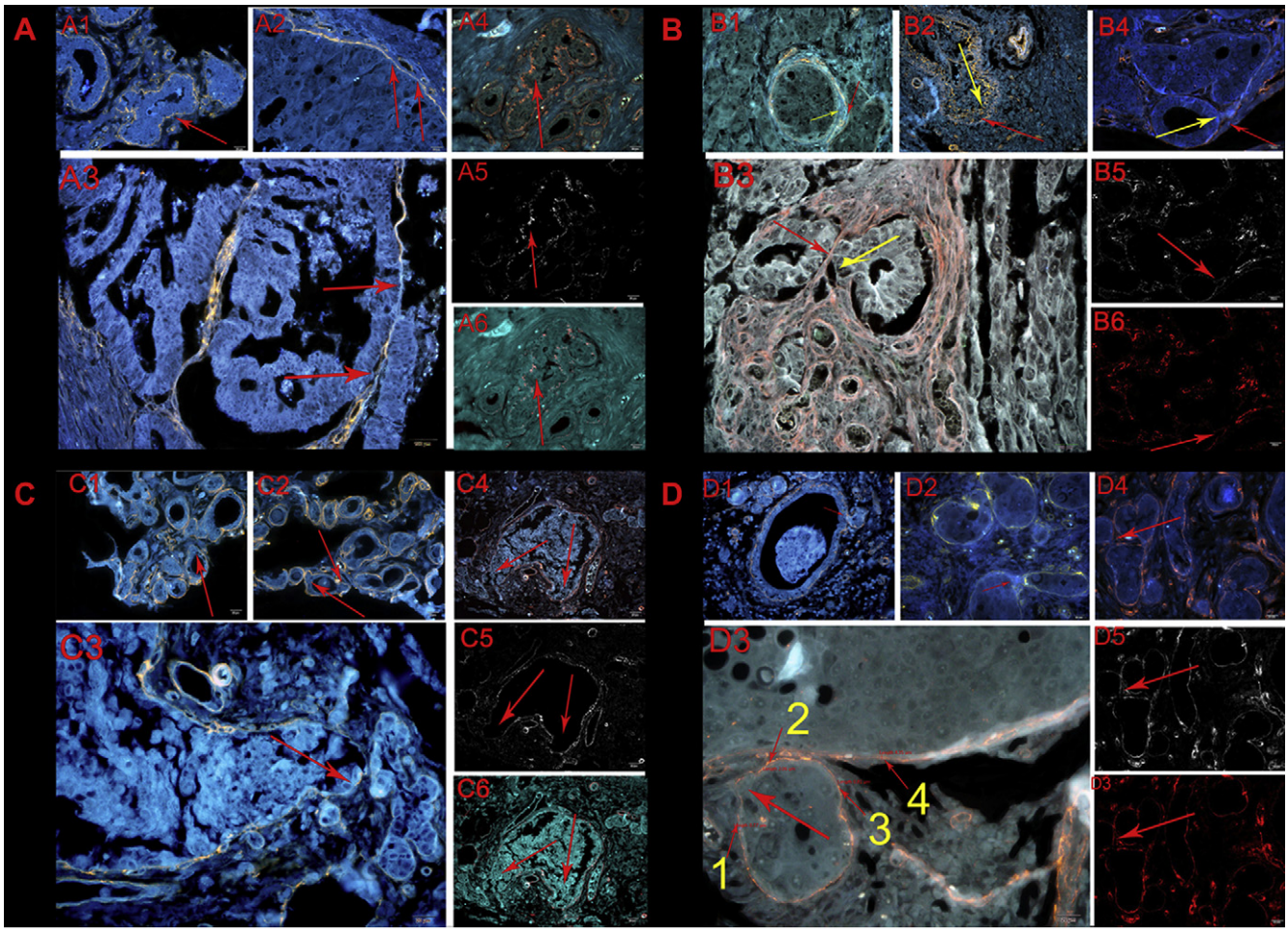

Fig. 3. Patterns of invasion. (A) Washing Pattern. (A1–A3) Washing pattern in breast cancer (A1, A2) and gastric cancer (A3). (A4–A6) Spectrum analysis of washing pattern in breast cancer including (A4) fluorescent image, (A5) spectral signal of QDs-585 extracted from (A4), and (A6) unmixed image. In this pattern, the ECMB becomes unsmooth (A1, Red arrow) and thinner at some sites (A2, A3, Red arrows), but remains continual and structurally intact. Magnification: 100× (A3), 400× (A1, A2, A4, A5, A6); Scale bar: 100 μm (A3), 20 μm (A1, A2 A4, A5, A6). (B) Ameba-like Pattern. (B1–B3) Ameba-like pattern in breast cancer (B1, B2) and gastric cancer (B3). (B4–B6) Spectrum analysis of Ameba-like pattern in breast cancer including (B4) fluorescent image, (B5) spectral signal of QDs-585 extracted from (B4), and (B6) unmixed image. In this pattern, the inner layer of ECMB at one site is degraded, and cancer cells invade into the ECMB (Yellow arrows) but the outer layer of ECMB remains continual and intact (Red arrows). With the spectrum imaging, the ECMB is shown more clearly that an invasion space is created due to type IV collagen degradation. Magnification: 400× (B1, B3, B4–B6), 200× (B3); Scale bar: 20 μm (B1, B3, B4–B6), 50 μm (B3). (C) Polarity Pattern. (C1–C3) Polarity pattern in breast cancer. (C4–C6) Spectrum analysis of polarity pattern in breast cancer including (C4) fluorescent imaging, (C5) spectral signal of QDs-585 extracted from (C4), and (C6) unmixed image. In this pattern, type IV collagen in the tumor-invasion front polarity is disrupted (Red arrows). However, the ECMB remains continual and intact. There may be more than one polarity in a cancer nest (C2, C4, C5, C6). Magnification: 400× (C1–C6); Scale bar: 20 μm (C1–C6). (D) Linear Pattern. (D1–D3) Linear pattern in breast cancer. (D4–D6) Spectrum analysis of linear pattern in breast cancer, including (D4) fluorescent imaging, (D5) spectral signal of QDs-585 extracted from (D4), and (D6) unmixed image. In this pattern, fibers of type IV collagen have multiple proteolytic foci (the thickness of ECMB in the areas of 1, 2, 3 and 4 is 0.77 μm, 2.06 μm, 0.86 μm and 4.35 μm, respectively) but eventually become clipped at a single site, thereby the invading cancer cells migrate in one direction mainly along a line (Red arrows). In other areas the ECMB remains continual and intact. Magnification: 400× (D1–D3); Scale bar: 20 μm (D1–D3).

visualization or emphasis. The QDs fluorescence signal information of cubes for each slide was analyzed by the image analysis software package (CRi Nuance) within the Nuance system. The fluorescent signal intensity and distribution areas of QDs probes in cancer tissues were calculated based on spectral unmixing. Feature extraction and pattern recognition algorithms were used to identify areas of interest and whole slide. Biomarker expressions in these identified areas were quantified by pixel-based intensity measurement, with a computer-generated threshold obtained from experimental data and was used for background subtraction.

3. Results

3.1. Fluorescent staining and spectrum analysis of ECMB

In this study, the ECMB constraining the cancer cells was visualized by staining type IV collagen, the most abundant constituent of the ECM, with QDs-585 probe in breast cancer (Fig. 1A1–A3) and gastric cancer (Fig. 1B1–B3) tissues. It has been observed that the ECMB is an amorphous, dense, and sheet-like structure of 1.85 μm–63.52 μm in thickness. The spatial relationship between cancer cells and type IV collagen in the ECMB indicates that cancer cells may contact the ECMB closely (Fig. 1A3) or away from the ECMB (Fig. 1B3). The loss of local constraints in tumor microenvironment can be quantitatively measured at the micrometer level. ECMB becomes thinner at the sites of potential cancer invasion. Furthermore, the properties of type IV collagen around the bounder of each cancer nest, such as continuity, smoothness, integrity and thickness can be well defined more clearly by spectrum analysis (Fig. 2A1 and B1). These features combined could help define the spatial relationship between cancer cells and stroma. Spectrum analysis is a new method to provide more accurate information than conventional fluorescent techniques. With the unique advantage of QDs, the spectrum of collagen around the cancer cells could be extracted accurately. Hiding points of ECMB degradation could be discovered even though ECMB itself appeared structurally intact (Fig. 2B3 and C3). The CRi Nuance software automatically separates the slide into 1336 ROI (region of interest), and the total signal of the slide is 214657.2 (Fig. 2C5). The loss of ECMB could be calculated by quantifying the signal of type IV collagen at different areas of ECMB. In the suspected area 1 of ECMB degradation (Red arrows), the total signal (390.298) is lower than in area 2 (749.838) (Fig. 2C4).

3.2. Patterns of invasion

We studied the spatial relationship between cancer cells and stroma at tumor-invasion front with combined imaging method of type IV collagen we had established. Four patterns of invasion with distinctive cancer cell-stroma interactions were observed, including washing pattern, ameba-like pattern, polarity pattern and linear pattern (Fig. 3). All patterns were summarized by fluorescence imaging (3 micrographs on the left column of each figure) and validated by spectrum analysis (3 micrographs on the right column of each figure). In the washing pattern (Fig. 3A), cancer cells erase ECMB everywhere without specific degradation focus, like waves brushing the dike on the beach. The ECMB becomes unsmooth and thinner, but remains structurally continual and intact. In the ameba-like pattern (Fig. 3B), after breaking the inner layer of ECMB, cancer cells invade into ECMB along the inner space of collagen on both sides to form an ameba-ulcer like invasion tunnel. The outer layer of ECMB remains continual and intact. In the polarity pattern (Fig. 3C), cancer cells proliferate with polarity, and the collagen at the tumor-invasion front is compressed and hydrolyzed to reduce the ECMB, forming a potential invasion tunnel. The ECMB diminishes and becomes progressively thinner in

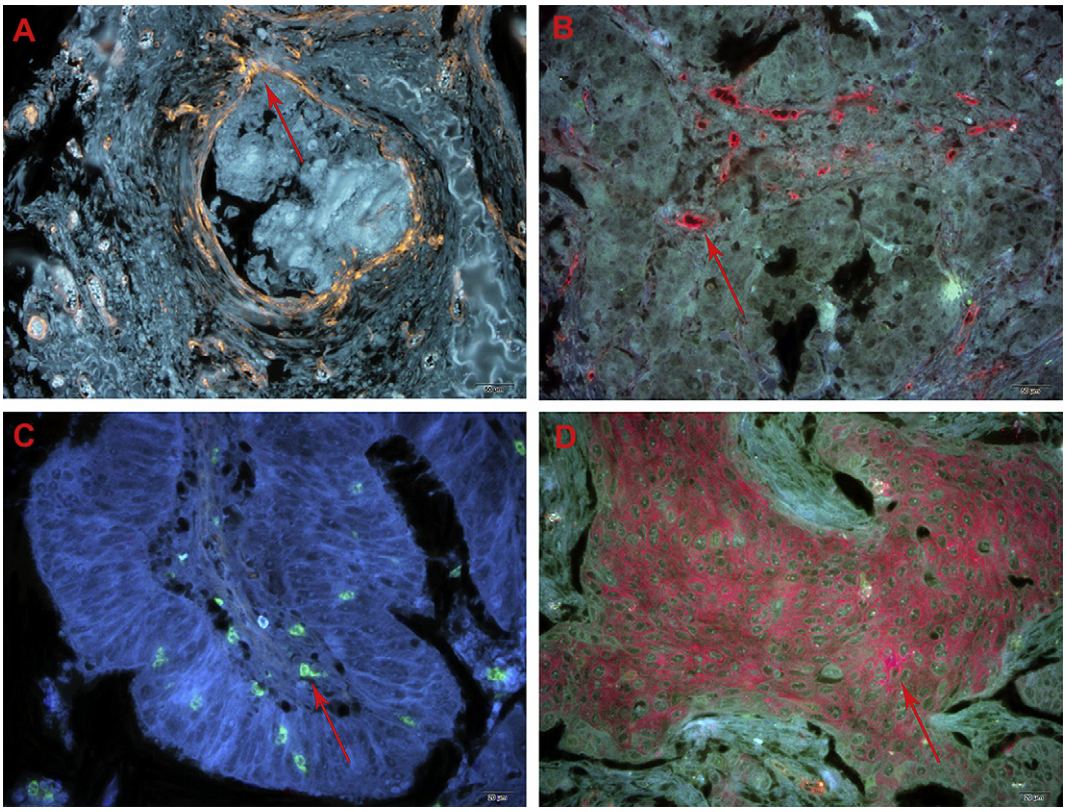

Fig. 4. QDs-based fluorescent imaging of important components in tumor microenvironment. (A) Type IV collagen recognized by QDs-585 conjugated antibody nano-probe (Red arrow). (B) Neovessels stained by QDs-655 conjugated anti-CD105 antibody recognizing endothelial cells (Red arrow). (C) Infiltrating macrophages stained by QDs-525 conjugated nano-probe (Red arrow). (D) MMP9 stained by QDs-655 conjugated nano-probe (Red arrow). MMP9 is mainly expressed in the cytoplasm of cancer cells. Magnification: 200× (A, B), 400× (C, D); Scale bar: 50 μm (A, B), 20 μm (C, D).

the polarity. In the linear pattern (Fig. 3D), cancer cells hydrolyze the ECMB at one focal point, gain access into the ECMB, and create a line of invasion pathway. Type IV collagen breaks down abruptly at a point, through which only a few cancer cells cross (Fig. 3D). Occasionally, invasion may have already occurred before the ECMB degradation becomes evident (Fig. 3D4–D6).

3.3. Immunolabelling of components in tumor microenvironment

To simultaneously evaluate the dynamic changes in tumor microenvironment during cancer progression, this study focused on major components of tumor microenvironment related to cancer invasion, including type IV collagen (Fig. 4A), endothelial cells (Fig. 4B), macrophages (Fig. 4C), and tissue destructive proteolytic enzymes MMP9 (Fig. 4D), all of which are important components of tumor stroma and involved in the ECM remodeling, tumor angiogenesis, and immune cell infiltration.

3.4. Multiplexed QDs imaging

In order to simultaneously visualize these components in tumor microenvironment and gain new insights into the complex interaction between cancer cells and stroma, we established a multiplexed QDs imaging method (Fig. 5). For spectrum analysis, different colors of QDs can be simultaneously excited by ultraviolet light and there is no spectral overlapping (Fig. 5D). Tumor angiogenesis, macrophages infiltration and the ECM remodeling were visualized more clearly and accurately in the ECM between two gastric cancer glands with spectrum analysis (Fig. 5A1–C2). The new method makes it possible to analyze the spatiotemporal process of invasion, and to reveal features of cancer invasion.

Several histopathological features were revealed by multiplexed QDs imaging. First, MMP9 is mainly expressed near the ECM where macrophages infiltrated, but ECMB maintains continual (Fig. 6A1 and A2). Second, ECM undergoes compression and remodeling before being broken, accompanied with tumor angiogenesis and macrophages infiltration at the leading edge (Fig. 6B1 and B2; Fig. 7A1 and A2). Third, tumor angiogenesis occurs hand in hand with ECMB degradation, however, when the ECMB is lost, no neovessels is found (Fig. 6C1 and C2). Fourth, high density of macrophages and neovessels are observed at the interface of tumor nest and stroma (Fig. 6D1 and D2). Another remarkable finding is that tumor angiogenesis may occur in tumor parenchyma near the infiltrating macrophages (Fig. 6D3). Fifth, the perivascular ECM is degraded at the interface with cancer cells, cancer cells intravasate into the vessels even though the ECMB is continual (Fig. 7A1 and A2). Interesting, macrophages of bone marrow-derived cells (BMDCs) extravasate from the vessels at the same point at the same time (Fig. 7B1 and B2).

3.5. The co-evolution of cancer cells and tumor stroma

Multiplexed QDs imaging highlights the temporal co-evolution between cancer cells and ECMB in each invasion pattern that can not be evaluated by single staining. In the washing pattern, successive waves of cancer cells induce progressive conditioning of the microenvironment to facilitate cancer cells spreading along a plane rather than deep penetration. Tumor angiogenesis is the

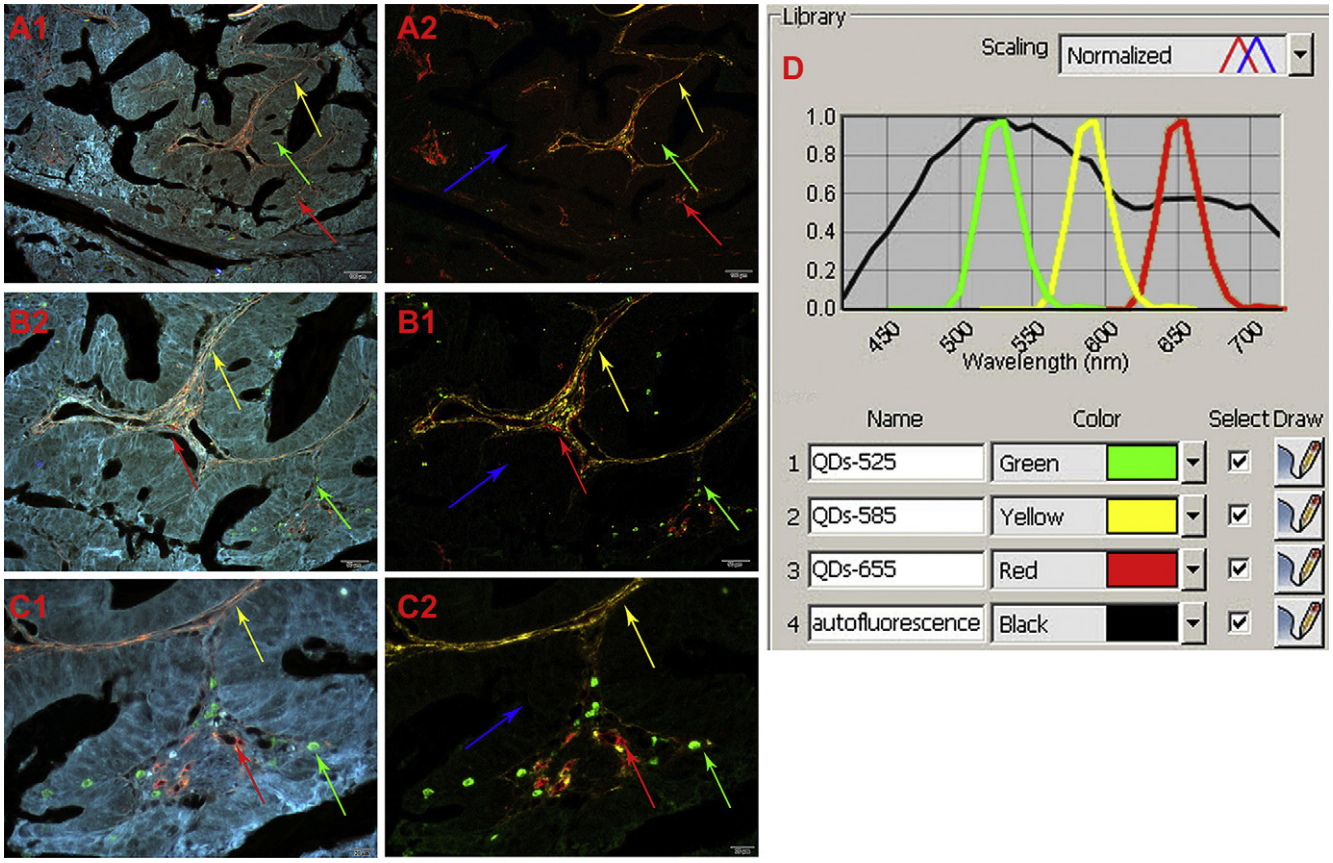

Fig. 5. The establishment of multiplexed QDs imaging and spectrum analysis. (A1, B1, C1) Infiltrating macrophages (Green arrows), type IV collagen (Yellow arrows) and neovessels (Red arrows) are labeled simultaneously in gastric cancer tissues with nano-probes QDs-525, QDs-585 and QDs-655, respectively. (A2, B2, C2) Corresponding unmixed image of (A1, B1, C1) obtained by spectrum analysis with differentiable autofluorescence (Blue arrows). (D) QD emission spectra and tissue autofluorescence data used for unmixed image. Magnification: 100× (A1, A2), 200× (B1, B2), 400× (C1, C2); Scale bar: 100 μm (A1, A2); 50 μm (B 1, B2); 20 μm (C1, C2).

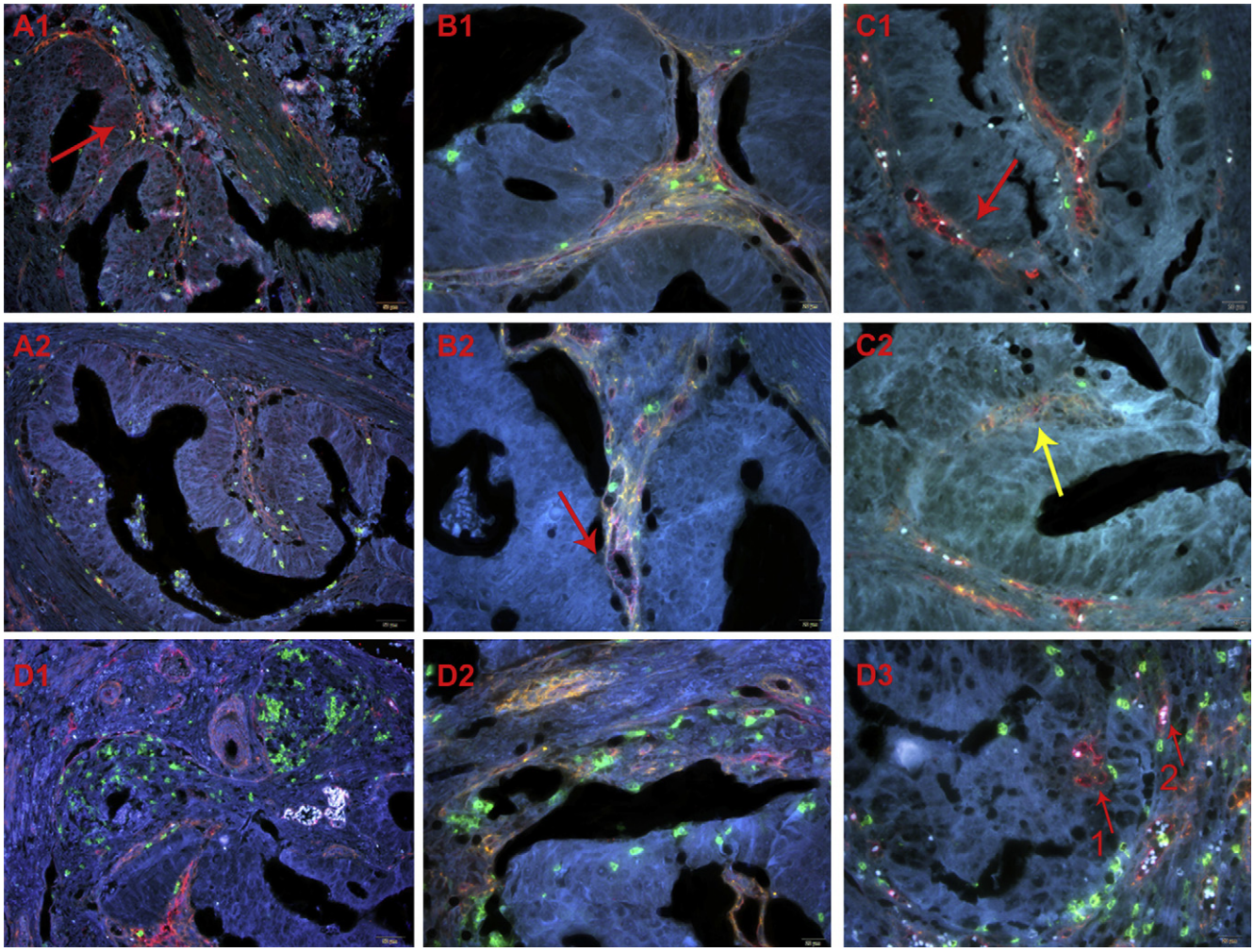

Fig. 6. Histopathological features of tumor microenvironment in the process of cancer invasion. (A1, A2) Multiplexed imaging of MMP9 (Red), type IV collagen (Yellow) and infiltrating macrophages (Green). MMP9 is expressed mainly in the area of macrophages infiltration. ECMB remains continual and intact. (B1–D3) Multiplexed imaging of neovessels (Red), type IV collagen (Yellow) and infiltrating macrophages (Green) to reveal features of cancer invasion. (B1, B2) Macrophages infiltration and tumor angiogenesis are two prominent features in the stroma where type IV collagen is degraded. Cancer cells contact with the type IV collagen around the neovessels. (C1, C2) Tumor angiogenesis occurs hand in hand with ECMB degradation (Red arrows). However, when the ECMB is lost, angiogenesis cease to occur (Yellow arrows). (D1, D2) High density of macrophages and neovessels are observed at the juncture of cancer cells and stroma where BM integrity was broken. (D3) Tumor angiogenesis may occur in tumor parenchyma near the infiltrating macrophages. The diameter of neovessel 1 in tumor parenchyma is 6.99 μm. The diameter of neovessel 2 at the juncture of cancer cells and stroma is 16.54 μm, containing 4 erythrocytes. Magnification: 200× (A1, A2, D1), 400× (B1, B2, C1, C2, D2, D3); Scale bar: 50 μm (A1, A2, D1), 20 μm (B1, B2, C1, C2, D2, D3).

major event in cancer progression (Fig. 8A). In the ameba-like pattern, extensive changes of tumor microenvironment may have occurred in the adjacent tissue even though the local tumor border is intact. Corresponding to the cancer cells invasion, type IV collagen in the inner layer of ECMB is broken and macrophages infiltration and tumor angiogenesis appear at the leading area (Fig. 8B). In the linear pattern, a few coordinated "pioneering cancer cells" form deep penetrating invasion tunnels along a line, paving the way for follower cancer cells. In this process, cancer cells would finally intravasate into neovessels, which is the hallmark in cancer progression (Fig. 8C). In the polarity pattern, simultaneous coordinated polarization of cancer cells at the leading edge of tumor front may cooperate in invasion by constantly changing the local microenvironment. Macrophages infiltration and tumor angiogenesis coexist with ECMB remodeling (Fig. 8D).

4. Discussion

Cancer progression is not an entirely cell-autonomous process. Instead, Darwinian evolution of tumors and resulting clinical progression are influenced, and perhaps even driven, by changes that occur in the tumor microenvironment [18]. A seminal event in cancer progression is cancer invasion, the ability of the neoplastic cells to transmigrate the surrounding extracellular matrix barriers while orchestrating a host stromal response that ultimately supports tissue-invasive and metastatic processes [4]. Structure and molecules are determinants in cancer progression [19]. Although the molecular mechanism of individual cell migration in the process of invasion was intensively studied [1], the architectural changes are only now beginning to be understood. Using conventional H&E staining and cancer nest borderline mapping, Friedl et al. summarized the structural changes of collective cancer cell migration as sheets, strands, clusters or ducts [20,21]. However, the real dynamic interactions of cancer cell-stroma are poorly understood in terms of temporal and spatial changes of the tumor microenvironment.

Unlike most other collagens, type IV collagen is an exclusive constitute of the basement-membrane and through a complex inter- and intra-molecular interactions form supramolecular networks to influence cell adhesion, migration, and differentiation [6]. Using combined imaging method of type IV collagen, we here

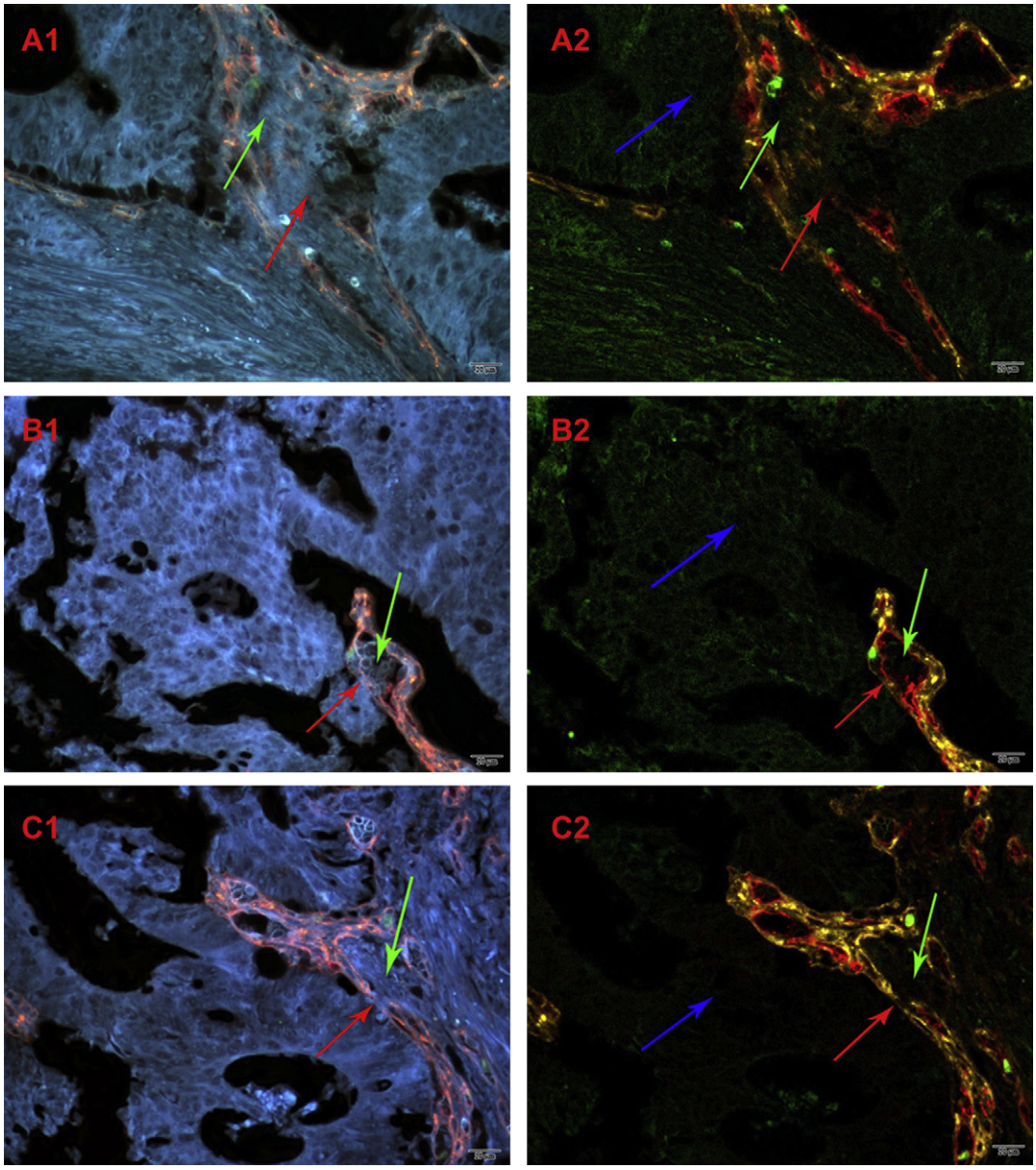

Fig. 7. Multiplexed QDs imaging indicates the co-evolution of cancer cells and tumor microenvironment. (A1, B1, C1) Multiplexed imaging of neovessels (Red), type IV collagen (Yellow) and infiltrating macrophages (Green). (A2, B2, C2) Corresponding unmixed image of (A1, B1, C1) obtained by spectrum analysis with distinctive autofluorescence background (Blue arrows). (A1, A2) Cancer cells migrate toward the area rich in macrophages and neovessels, and ECMB is compressed and degraded at the leading edge (Red arrows). Some cancer cells have transmigrated the ECMB as the continuality of ECMB is lost (Green arrows). (B1, B2) Type IV collagen is degraded at the interface of cancer cells and perivacular ECMB (Red arrows). Cancer cells intravasate into the vascular even though the ECMB is continual (Green arrows). In addition, macrophages extravasate into the ECMB from the vascular. (C1, C2) Several cancer cells have invaded into the ECMB (Green arrows), and some cancer cells are crossing the ECMB (Red arrows). Magnification: 400× (A1–C2); Scale bar: 20 μm (A1–C2).

report a new method to study the spatial relationship between cancer cells and stroma at tumor-invasion front. With the unique advantages of QDs, the properties of type IV collagen around the bounder of each cancer nest, such as continuity, smoothness, integrity and thickness can be well defined. In addition, the loss of local constraints in tumor microenvironment can be quantitatively measured. Four patterns of invasion with distinctive cancer cell–stroma interactions were observed, including washing pattern, ameba-like pattern, polarity pattern and linear pattern. In the washing pattern, successive waves of cancer cells induce progressive conditioning of the microenvironment to facilitate cancer cells spreading along a plane rather than deep penetration. In the ameba-like pattern, extensive tissue destruction may have occurred in the adjacent tissue even though the local tumor border was intact. Therefore, invasive tunnels may have already developed beneath the seemly intact tumor margin. In the polarity pattern, simultaneous coordinated polarization of cancer cells at the leading edge of tumor front may cooperate in invasion by constantly changing the local microenvironment. In the linear pattern, a few coordinated "pioneering cancer cells" form deep penetrating invasion tunnels along a line, paving the way for follower cancer cells. Two models of invasion were hypothesized according to the ECMB status that indicates the spatial variation in cancer progression, including barrier evasion model and barrier failure model, that similar to our results [18]. But more details were revealed in our study. Briefly, barrier failure model like the washing pattern, while barrier evasion model is similar to the other patterns in our study. Among these four patterns, washing pattern may correlate with best prognosis as

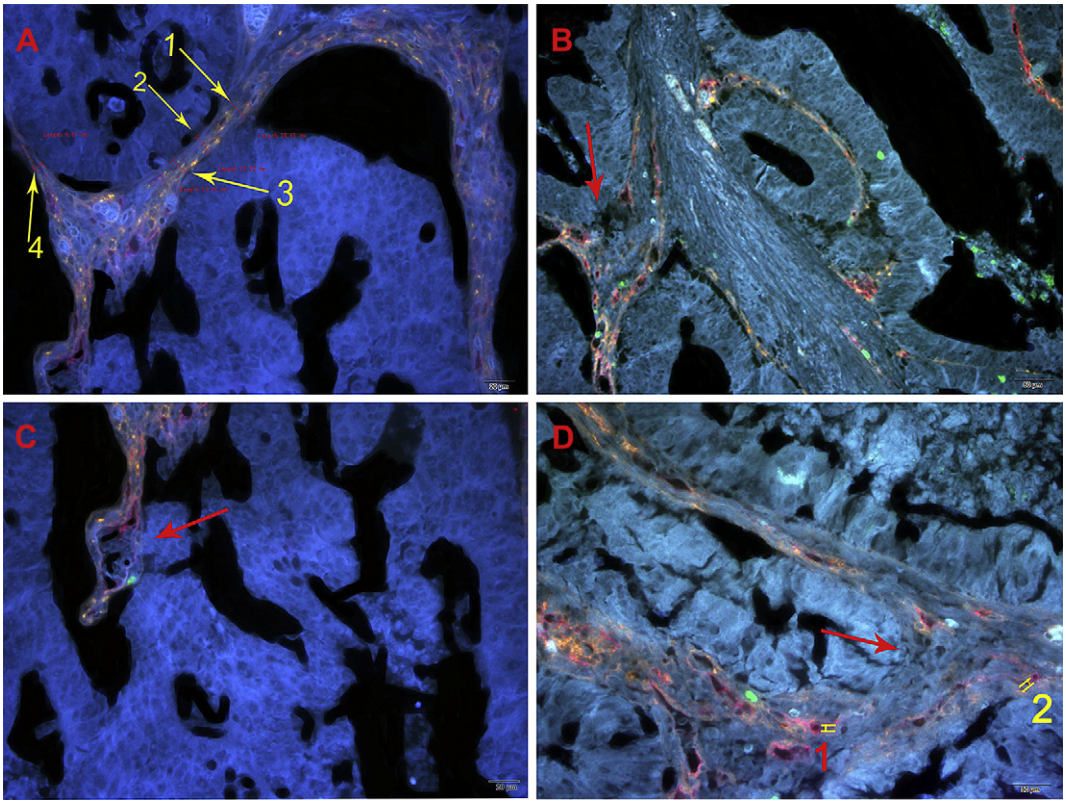

Fig. 8. The features of four patterns of invasion identified by incorporating the temporal dimension. (A) Washing Pattern. The ECMB is degraded and becomes thinner that similar to the results in Fig. 3. The thickness of ECMB at areas 1, 2, 3, and 4 is 18.65 μm, 12.88 μm, 10.96 μm and 6.67 μm, respectively. Though the ECMB is still continual, lots of neovessels appear in the ECMB. (B) Ameba-Like Pattern. The inner layer of ECMB is broken accompanied with tumor angiogenesis. Cancer cells migrate along the fibers toward the direction rich in macrophages and neovessels. (C) Linear Pattern. Cancer cells directly invade into the neovessel, the diameter of which is less than 20 μm (Scale bar, 20 μm). Macrophages extravasate from the vessels. No type IV collagen is visible in the contact surface. (D) Polarity Pattern. Cancer cells proliferate with polarity, and ECMB is degraded at the leading edge. Macrophages infiltration and tumor angiogenesis coexist with ECMB remodeling which is not failed. Magnification: 400× (A, C), 200× (B, D); Scale bar: 20 μm for (A, C); 50 μm for (B, D).

crossing ECMB occurs relatively late. In contrast, linear pattern may reflex the worst prognosis because cancer cells may have already deeply penetrated the ECM in spite of the density of the surrounding type IV collagen and such cancer may have already become a potentially systemic disease even it is diagnosed as early stage by conventional pathology. By cleaving collagen fibers and re-patterning them into parallel bundles, individual cells reorient the ECM to permit movement in tunnel-like microtracks. Cells along the edge of these tunnels can excavate ECM outward, generating macrotracks through which collective mass movement of cancer cells can occur [22].

The formation of a clinically relevant tumor requires support from the surrounding normal stroma, also referred to as the tumor microenvironment [23]. Carcinoma-associated fibroblasts, leukocytes, BMDCs, blood and lymphatic vascular endothelial cells present within the tumor microenvironment contribute to tumor progression. Tumor microenvironment varies temporally and plays different roles in different stages of cancer. It has been evident that although cancer cells and some traditionally proteins account for invasion and metastasis are no different, the primary tumor microenvironment, the invasive microenvironment and the metastatic microenvironment are different [24]. In the temporal variation of tumor microenvironment, tumor angiogenesis, ECM remodeling and immune cell infiltration are critical events in the cancer progression.

Although the critical role of the dynamic and reciprocal interactions between tumor cells and their microenvironment has been documented, such study performed by incorporating solitude study as the simultaneous visualization of those essential events is impossible for technical barrier. In our preliminary study, the co-evolution process was evaluated by staining MMP9, macrophages, type IV collagen and endoglin (CD105), respectively [25]. Multiplexed imaging, which holds the great promise to overcome the barrier, allows high degree of sensitivity and selectivity in cancer imaging with multiple antigens that are not available from traditional H&E and IHC [26]. QDs is a new class of nanopartical probe showing the potential to revolutionize biological imaging, including multiplexed imaging, due to their intense fluorescent signals and multiplexing capabilities [9,27]. This study established a novel protocol for QDs-based multiplexed imaging on complex clinical cancer tissues. Different colors of QDs were simultaneously excited by a single light source, with minimal spectral overlapping. Multiplexed QDs imaging permits not only the visualization of the spatial but also the temporal process of the co-evolution of cancer cells and their microenvironment.

This study takes a holistic approach to investigating such variations in tumor microenvironment during cancer invasion. In addition to studying the invading cancer cells, major players in the tumor microenvironment are also closely identified and studied concurrently, by QDs-based simultaneous quantitative imaging of major constitutes of ECMB (collagens, tumor infiltrating macrophages, MMPs and tumor angiogenesis). Such an approach could help us look at the picture of cancer invasion from the perspectives of not only cancer cells but also their microenvironment, gaining new insights into this complex and critical cancer event. Five histopathological properties were suggested by multiplexed QDs

imaging. Though those properties may exist in the four patterns of invasion mentioned above, which were summarized only by analyzing the spatial relationship between cancer cells and stroma, the four patterns are different incorporation of the temporal dimension. In the washing pattern, tumor angiogenesis is the major event in cancer progression. While in the polarity pattern, macrophages infiltration and tumor angiogenesis coexist with ECMB remodeling but not failure. In the ameba-like pattern, type IV collagen is broken and macrophages infiltration and tumor angiogenesis coexist. In the linear pattern, intravasation into neovessels is the hallmark in cancer progression.

All the results indicate the co-evolution of cancer cells and tumor microenvironment that can not be explained by the variation of only one component. Although it has been poorly understood tissue dynamics that shift cell and ECM interfaces during collective invasion, invasive growth in the absence of active invasion, study focused on cell migration demonstrated that the process of ECM regression in response to an expanding cell compartment is consistent with the MMP dependence of many cancers during progression [28,29]. At the same time, work in the field of mechanical biology has revealed that many cell behaviors critical for cancer formation (e.g., growth, differentiation, motility, apoptosis) can be controlled by physical interactions between cells and their ECM adhesions that alter the mechanical force balance in the ECM, cell and cytoskeleton [30]. Epithelial tumor progression also can be induced in vitro by changing ECM mechanics or altering cytoskeletal tension generation through mediate control of capillary cell growth and angiogenesis, which are equally critical for cancer progression and metastasis [31,32]. Tumor angiogenesis is the process of new blood vessel formation which is regarded as one of the hallmark of cancer growth and metastasis. Tumor angiogenesis is tightly regulated by a balance between endogenous proangiogenic and antiangiogenic factors to maintain homeostasis in tissue [33–35]. ECM can promote tumor angiogenesis by releasing matrix-bound growth factors that inherent to those processes. However, ECMB acts as a repository not only for growth factors, but also for antiangiogenic factors. The noncollagenous domain 1 (NC1 domain) is the C-terminal domain of collagen. In several types of collagen, proteolytic cleavage from the parent molecule can release the NC1 domain that can inhibit tumor angiogenesis. Furthermore, the NC1 domain can also exert adhesive, promigratory, proapopotic and survival effects [36,37]. Angiogenesis may not occur when there is rich in NC1 domain as a result of the complete degradation of the ECM. Apart from the non-cell factor, parenchymal, endothelial cells, and immune cells present within the tumor microenvironment contribute to tumor progression, including angiogenesis [5]. Tumor-associated macrophages (TAMs) are a prominent inflammatory cell population in many tumor types residing in both perivascular and avascular, hypoxic regions of these tissues [38]. Analysis of TAMs in human tumor biopsies has shown that they express a variety of tumor-promoting factors and evidence from transgenic murine tumor models has provided unequivocal evidence for the importance of these cells in driving hypoxia, angiogenesis, lymphangiogenesis, immunosuppression, and metastasis [39,40].

5. Conclusion

The microenvironment within a tumor represents a complex dynamic exchange between cancer cells and their surrounding stroma which requires carefully designed models in order to understand the role of its stromal components in carcinogenesis, tumor progression, invasion, and metastasis. Lack of suitable models that faithfully reproduce the normal tissue architecture and microenvironments poses a challenge for functional studies aimed at testing hypotheses built based on observations in human tissues. We have developed here an imaging method, based on the powerful properties of QDs, to study the co-evolution of cancer cells and tumor stroma at the architectural level. We have identified four patterns of tumor invasion by incorporating the temporal and spatial dimensions. Multiplexed QDs imaging should enhance the development of preventative and therapeutic interventions that specifically target microenvironmental alterations.

Acknowledgments

This work is supported by The Science Fund for Creative Research Groups of the National Natural Science Foundation of China (No. 20621502, 20921062), Foundation for the Author of National Excellent Doctoral Dissertation of PR China (FANEDD-200464) and “the Fundamental Research Funds for the Central Universities” (No. 4103005) of Ministry of Education of China.

Appendix

Figures with essential color discrimination. All the figures in this article may be difficult to interpret in black and white. The full color images can be found in the on-line version, at doi:10.1016/j.biomaterials.2010.12.053.

References

[1] Wolf K, Wu YI, Liu Y, Geiger J, Tam E, Overall C, et al. Multi-step pericellular proteolysis controls the transition from individual to collective cancer cell invasion. Nat Cell Biol 2007;9(8):893–904.
[2] Xu R, Boudreau A, Bissell MJ. Tissue architecture and function: dynamic reciprocity via extra- and intra-cellular matrices. Cancer Metastasis Rev 2009;28(1–2):167–76.
[3] Albini A, Sporn MB. The tumour microenvironment as a target for chemoprevention. Nat Rev Cancer 2007;7(2):139–47.
[4] Rowe RG, Weiss SJ. Navigating ECM barriers at the invasive front: the cancer cell-stroma interface. Annu Rev Cell Dev Biol 2009;25:567–95.
[5] Polyak K, Haviv I, Campbell IG. Co-evolution of tumor cells and their microenvironment. Trends Genet 2009;25(1):30–8.
[6] Kalluri R. Basement membranes: structure, assembly and role in tumour angiogenesis. Nat Rev Cancer 2003;3(6):422–33.
[7] Johann DJ, Rodriguez-Canales J, Mukherjee S, Prieto DA, Hanson JC, Emmert-Buck M, et al. Approaching solid tumor heterogeneity on a cellular basis by tissue proteomics using laser capture microdissection and biological mass spectrometry. J Proteome Res 2009;8(5):2310–8.
[8] Heppner GH, Miller BE. Tumor heterogeneity: biological implications and therapeutic consequences. Cancer Metastasis Rev 1983;2(1):5–23.
[9] Liu J, Lau SK, Varma VA, Moffitt RA, Caldwell M, Liu T, et al. Molecular mapping of tumor heterogeneity on clinical tissue specimens with multiplexed quantum dots. ACS Nano 2010;4(5):2755–65.
[10] Pelley JL, Daar AS, Saner MA. State of academic knowledge on toxicity and biological fate of quantum dots. Toxicol Sci 2009;112(2):276–96.
[11] Resch-Genger U, Grabolle M, Cavaliere-Jaricot S, Nitschke R, Nann T. Quantum dots versus organic dyes as fluorescent labels. Nat Methods 2008;5(9):763–75.
[12] Chen LD, Liu J, Yu XF, He M, Pei XF, Tang ZY, et al. The biocompatibility of quantum dot probes used for the targeted imaging of hepatocellular carcinoma metastasis. Biomaterials 2008;29(31):4170–6.
[13] Gokarna A, Jin LH, Hwang JS, Cho YH, Lim YT, Chung BH, et al. Quantum dot-based protein micro- and nanoarrays for detection of prostate cancer biomarkers. Proteomics 2008;8(9):1809–18.
[14] Chen C, Peng J, Xia HS, Yang GF, Wu QS, Chen LD, et al. Quantum dots-based immunofluorescence technology for the quantitative determination of HER2 expression in breast cancer. Biomaterials 2009;30(15):2912–8.
[15] Chen C, Xia HS, Gong YP, Peng J, Peng CW, Hu MB, et al. The quantitative detection of total HER2 load by quantum dots and the identification of a new subtype of breast cancer with different 5-year prognosis. Biomaterials 2010;31(33):8818–25.
[16] Ben-Ari ET. Nanoscale quantum dots hold promise for cancer applications. J Natl Cancer Inst 2003;95(7):502–4.
[17] Michalet X, Pinaud FF, Bentolila LA, Tsay JM, Doose S, Li JJ, et al. Quantum dots for live cells, in vivo imaging, and diagnostics. Science 2005;307(5709):538–44.
[18] Polyak K, Kalluri R. The role of the microenvironment in mammary gland development and cancer. Cold Spring Harb Perspect Biol; 2010;. doi:10.1101/cshperspect.a003244.

[19] Friedl P, Wolf K. Plasticity of cell migration: a multiscale tuning model. J Cell Biol 2010;188(1):11–9.
[20] Friedl P, Gilmour D. Collective cell migration in morphogenesis, regeneration and cancer. Nat Rev Mol Cell Biol 2009;10(7):445–57.
[21] Friedl P, Maaser K, Klein CE, Niggemann B, Krohne G, Zanker KS. Migration of highly aggressive MV3 melanoma cells in 3-dimensional collagen lattices results in local matrix reorganization and shedding of alpha2 and beta1 integrins and CD44. Cancer Res 1997;57(10):2061–70.
[22] Friedl P, Wolf K. Tube travel: the role of proteases in individual and collective a cancer cell invasion. Cancer Res 2008;68(18):7247–9.
[23] Hu M, Polyak K. Microenvironmental regulation of cancer development. Curr Opin Genet Dev 2008;18(1):27–34.
[24] Joyce JA, Pollard JW. Microenvironmental regulation of metastasis. Nat Rev Cancer 2009;9(4):239–52.
[25] Peng CW, Liu XL, Liu X, Li Y. Co-evolution of cancer microenvironment reveals distinctive patterns of gastric cancer invasion: laboratory evidence and clinical significance. J Transl Med 2010;8(1):101.
[26] Dubertret B, Skourides P, Norris DJ, Noireaux V, Brivanlou AH, Libchaber A. In vivo imaging of quantum dots encapsulated in phospholipid micelles. Science 2002;298(5599):1759–62.
[27] Wu X, Liu H, Liu J, Haley KN, Treadway JA, Larson JP, et al. Immunofluorescent labeling of cancer marker Her2 and other cellular targets with semiconductor quantum dots. Nat Biotechnol 2003;21(1):41–6.
[28] Coussens LM, Fingleton B, Matrisian LM. Matrix metalloproteinase inhibitors and cancer: trials and tribulations. Science 2002;295(5564):2387–92.
[29] Hotary KB, Allen ED, Brooks PC, Datta NS, Long MW, Weiss SJ. Membrane type I matrix metalloproteinase usurps tumor growth control imposed by the three-dimensional extracellular matrix. Cell 2003;114(1):33–45.
[30] Ingber DE. Can cancer be reversed by engineering the tumor microenvironment? Semin Cancer Biol 2008;18(5):356–64.
[31] Mammoto A, Huang S, Moore K, Oh P, Ingber DE. Role of RhoA, mDia, and ROCK in cell shape-dependent control of the Skp2-p27kip1 pathway and the G1/S transition. J Biol Chem 2004;279(25):26323–30.
[32] Paszek MJ, Zahir N, Johnson KR, Lakins JN, Rozenberg GI, Gefen A, et al. Tensional homeostasis and the malignant phenotype. Cancer Cell 2005;8(3):241–54.
[33] Folkman J. Angiogenesis. Annu Rev Med 2006;57:1–18.
[34] Kerbel RS. Molecular origins of cancer: tumor angiogenesis. N Engl J Med 2008;358(19):2039–49.
[35] Kleinman ME, Yamada K, Takeda A, Chandrasekaran V, Nozaki M, Baffi JZ, et al. Sequence- and target-independent angiogenesis suppression by siRNA via TLR3. Nature 2008;452(7187):591–7.
[36] Sudhakar A, Sugimoto H, Yang CQ, Lively J, Zeisberg M, Kalluri R. Human tumstatin land human endostatin exhibit distinct antiangiogenic activities mediated by alpha v beta 3 and alpha 5 beta 1 integrins. Proc Natl Acad Sci U S A 2003;100(8):4766–71.
[37] Mundel TM, Yliniemi AM, Maeshima Y, Sugimoto H, Kieran M, Kalluri R. Type IV collagen alpha 6 chain-derived noncollagenous domain 1 (alpha 6(IV)NC1) inhibits angiogenesis and tumor growth. Int J Cancer 2008;122(8):1738–44.
[38] Coffelt SB, Hughes R, Lewis CE. Tumor-associated macrophages: effectors of angiogenesis and tumor progression. BBA Rev Cancer 2009;1796(1):11–8.
[39] Luo YP, Zhou H, Krueger J, Kaplan C, Lee SH, Dolman C, et al. Targeting tumor-associated macrophages as a novel strategy against breast cancer. J Clin Invest 2006;116(8):2132–41.
[40] Sierra JR, Corso S, Caione L, Cepero V, Conrotto P, Cignetti A, et al. Tumor angiogenesis and progression are enhanced by Sema4D produced by tumor-associated macrophages. J Exp Med 2008;205(7):1673–85.